

Editorial Manager(tm) for Journal of Electronic Materials  
Manuscript Draft

Manuscript Number: JEMS-2105

Title: An Introduction to System Level Steady-State and Transient Modeling and Optimization of High Power Density Thermoelectric Generator Devices Made of Segmented Thermoelectric Elements

Article Type: S.I.: ICT2010

Keywords: thermoelectric; power generation; modeling; waste heat recovery; steady state; transient

Corresponding Author: Douglas Crane,

Corresponding Author's Institution: BSST LLC

First Author: Douglas Crane

Order of Authors: Douglas Crane

1  
2  
3  
4 An Introduction to System Level Steady-State and Transient Modeling and Optimization of High Power Density  
5  
6 Thermoelectric Generator Devices Made of Segmented Thermoelectric Elements  
7  
8  
9

10  
11 D.T. Crane  
12  
13

14  
15 BSST, LLC  
16  
17

18 5462 Irwindale Avenue  
19

20 Irwindale, CA 91706-2058 USA  
21

22 1-626-593-4532  
23

24 1-626-815-7441 (fax)  
25

26 dcrane@bsst.com  
27  
28  
29  
30

31 Abstract  
32  
33  
34  
35

36 High power density, segmented, thermoelectric (TE) elements have been intimately integrated into heat exchangers,  
37  
38 eliminating many of the loss mechanisms of conventional TE assemblies, including the ceramic electrical isolation  
39  
40 layer. Numerical models comprised of simultaneously solved, non-linear, energy balance equations have been  
41  
42 created to simulate these novel architectures. These models begin at the element level and progress to the device  
43  
44 and finally to the system level. Both steady state and transient models have been created in a MATLAB/Simulink  
45  
46 environment. The models predict data from experiments in various configurations and applications over a broad  
47  
48 range of temperature, flow, and current conditions for power produced, efficiency, and a variety of other important  
49  
50 outputs.  
51  
52

53  
54  
55  
56 The ability to accurately and precisely model such devices allows devices to be extensively studied without  
57  
58 additional experimentation. Using the validated models, the devices and systems can be optimized using advanced  
59  
60 multi-parameter optimization techniques for different operating conditions. Optimization objectives such as  
61  
62  
63  
64  
65

1  
2  
3  
4  
5  
6  
7  
8  
9  
10  
11  
12  
13  
14  
15  
16  
17  
18  
19  
20  
21  
22  
23  
24  
25  
26  
27  
28  
29  
30  
31  
32  
33  
34  
35  
36  
37  
38  
39  
40  
41  
42  
43  
44  
45  
46  
47  
48  
49  
50  
51  
52  
53  
54  
55  
56  
57  
58  
59  
60  
61  
62  
63  
64  
65

maximum power output, power density, and efficiency can be pursued with numerous different constraints being considered such as pressure drop and temperature limitations. Devices optimized for particular steady state conditions can then be dynamically simulated in a transient operating model. This transient model incorporates system and device thermal time constants that affect performance. The transient model can be operated for a variety of operating conditions including automotive and truck drive cycles.

1  
2  
3  
4  
5  
6  
7  
8  
9  
10  
11  
12  
13  
14  
15  
16  
17  
18  
19  
20  
21  
22  
23  
24  
25  
26  
27  
28  
29  
30  
31  
32  
33  
34  
35  
36  
37  
38  
39  
40  
41  
42  
43  
44  
45  
46  
47  
48  
49  
50  
51  
52  
53  
54  
55  
56  
57  
58  
59  
60  
61  
62  
63  
64  
65

## Key Words

thermoelectric, power generation, modeling, waste heat recovery, steady state, transient

## Introduction

In the last few years, there has been important work done in the area of thermoelectric (TE) power generation modeling. This work has included analyzing thermoelectric elements with finite element analysis (FEA)<sup>1, 2</sup>, which also involved the addition of a thermoelectric module to the finite element (FEA) package, ANSYS<sup>3</sup>. It has also comprised work done using the mathematical package SPICE for numerical modeling<sup>4-6</sup>. Quasi-steady state modeling of thermoelectric generators (TEG) integrated into automotive systems in ADVISOR was also conducted<sup>7</sup>.<sup>8</sup>. Numerical optimization studies have also been executed for segmented elements<sup>9</sup>. Hendricks et al.<sup>10-12</sup> have used stochastic and probabilistic approaches for optimization of advanced thermoelectric conversion systems. While this work has been important and has continued to improve the ability to predict TE performance, there is still room for further improvement.

The current work builds off of previous thermoelectric modeling work done in a MATLAB/Simulink environment<sup>13</sup>.<sup>14</sup>. Previous papers by the author have discussed modeling of thermoelectrics in heating and cooling<sup>15</sup>. They have also discussed initial modeling of the building blocks for power generation<sup>16</sup>. The current paper takes this previous work and extends the validated heating and cooling device and system level models to power generation and takes the validated building block models in power generation and extends those to device and system level models. These initial models are steady state models. Advanced optimization tools are discussed in relation to these models. With optimized designs in steady state for nominal design conditions, the TE models are further extended as the introduction of transient operating models are discussed. This paper is an introduction to these models. Full validation of these models is not complete yet, but what validation has been completed will be reported in the context of this paper.

1  
2  
3  
4  
5  
6  
7 Steady State Model Development  
8  
9

10  
11 The thermoelectric device being modeled in this paper is unique in its design as it integrates high power density TE  
12 material directly into the heat exchanger device. Different aspects of these designs have been described and  
13 discussed extensively in previous papers<sup>16-20</sup> and will only be summarized and generally discussed here.  
14  
15  
16  
17

18  
19  
20 Each TE element (alternating between p- and n- legs) is sandwiched between connectors or shunts as shown in  
21 Figure 1. These connectors serve as a means of both thermal and electrical energy transport. The connectors  
22 provide an electrical path from one TE element to another completing the necessary TE p-n couple. The connectors  
23 also provide a thermal path from the hot and cold fluid-carrying channels to the TE elements. The connectors are  
24 joined to the TE elements using a high electrical and thermal conductivity interface.  
25  
26  
27  
28  
29  
30

31  
32  
33 The shunts are connected to the channels carrying hot and cold fluids using high thermal conductivity and  
34 electrically isolating interfaces. The device is placed in compression separately in both the thermal and electrical  
35 flow directions. The benefits of this design concept, which are significant, have been elaborated in previous  
36 papers<sup>17, 18, 21, 22</sup> and will not be restated here.  
37  
38  
39  
40  
41

42  
43  
44 Previously introduced in Crane et al.<sup>16, 17</sup>, the equations used to model the TE elements were defined in Snyder<sup>23</sup>.  
45 Looking at the TE element in the direction of heat flow, a temperature gradient across the element is predefined.  
46 This temperature gradient is then subdivided into smaller equal temperature steps. The three basic thermoelectric  
47 material properties, Seebeck coefficient, electrical resistivity, and thermal conductivity, which are defined as  
48 functions of temperature, are calculated at each of these temperature steps across the entire temperature gradient.  
49 The reduced current density, which is the ratio of the electric current density to the conduction-driven heat flux<sup>23</sup> is  
50 calculated at each temperature step using the calculated TE material properties.  
51  
52  
53  
54  
55  
56  
57  
58  
59  
60  
61  
62  
63  
64  
65

1  
2 An initial reduced current density is defined as  
3  
4  
5

$$6 \quad u_1 = \frac{I}{Q_h - \alpha_1 I T_1}$$

7  
8  
9

10 Equation 1  
11  
12  
13

14 This equation is negative if an n-type material is being evaluated. The temperature variation along the length of the  
15 element is then calculated as a function of the reduced current density, with the sum being equal to the current  
16 density times element length<sup>23</sup>.  
17  
18  
19  
20  
21  
22

23 Using these now defined equations, the model makes initial assumptions for heat flow and current. Using the  
24 optimization function, FMINCON, in MATLAB, the model iteratively solves for the heat flow and current that  
25 maximizes TE element efficiency. A constraint for the optimization is that the TE elements must match a predefined  
26 element length. Another input to the model is the electrical resistance at the TE element interfaces. This resistance  
27 has been indirectly measured in validated TE heating and cooling experiments and is similar to those reported in the  
28 literature<sup>24</sup>. The thermal interfacial resistance is related to this electrical contact resistance using the Wiedmann-  
29 Franz law<sup>25</sup>. A reduced current density is also evaluated at the temperature step created by the electrical contact  
30 resistance and the temperature drop caused by the thermal contact resistance. In this way, the metallization and  
31 other interfacial attributes of the elements are evaluated. To model segmented or multi-material elements, more  
32 interfaces were added, but the evaluation method remained the same. Validation of this model was described for  
33 both single material and segmented material TE elements in Crane et al.<sup>16</sup>. This element and couple-level model was  
34 adjusted to fit into a larger model that integrated these TE elements into a TE device, including shunts, heat  
35 exchangers, and fluid flows.  
36  
37  
38  
39  
40  
41  
42  
43  
44  
45  
46  
47  
48  
49  
50  
51  
52  
53

54 Building on previous work of validated TE numerical simulation<sup>15</sup>, a MATLAB-based, numerical, steady-state  
55 model was created, comprised of simultaneously solved, non-linear, energy balance equations. These energy  
56 balance equations simulate the high-power density, segmented element TE assemblies discussed above. The  
57 numerical model of the TE heat exchanger uses a finite volume approach with discretization in the axial direction of  
58  
59  
60  
61  
62  
63  
64  
65

1  
2 both hot and cold flows. A first-order upwind differencing scheme is implemented for the convective derivatives.  
3  
4 Downwind differencing can also be chosen as an option. Transverse or radial heat transfer is modeled using  
5  
6 standard conduction equations that incorporate central differencing discretization for the gradients. Each segment of  
7  
8 the fluid-carrying channel is separated into four control volumes. Since the temperature gradients across each  
9  
10 segment and from one segment to another are small, this level of discretization was determined to be adequate.  
11  
12 Differential algebraic equations model the energy balances for each control volume.  
13  
14  
15  
16  
17

18 Convective heat transfer coefficient and pressure drop correlations were derived from experimental and simulation<sup>26</sup>  
19  
20 data. The thermal resistances of the device are rigorously modeled. These resistances include thermal contact  
21  
22 resistances at each TE element interface, including between different material segments of a segmented element as  
23  
24 well as the interfacial resistance between the TE element and the shunts on both the hot and cold side of the  
25  
26 elements. The metallization layer(s) on the elements are lumped into this contact resistance both thermally and  
27  
28 electrically. The thermal contact resistance is also simulated between the shunts and the heat exchangers.  
29  
30 Temperature drops are also calculated from the fluid through the fins to the wall of the heat exchanger. These drops  
31  
32 continue through the heat exchanger wall and through any interface materials, which can include electrically  
33  
34 insulating coatings such as anodize and thermal grease. The thermal resistance of the shunts, based on geometry and  
35  
36 material, are then accounted for culminating in a surface temperature at the metallization layer of the TE.  
37  
38  
39  
40  
41

42 Heat loss factors are also rigorously accounted for in the model. Convective, conductive, and radiative heat losses  
43  
44 are considered. Heat can be lost to the outside environment or it can be transferred from a hot surface to a cold  
45  
46 surface within the device or system. The geometry of the components is considered when determining where the  
47  
48 heat is being transferred to. Different environments can be modeled, including air, argon, xenon, or vacuum.  
49  
50 Different insulations can also be modeled, such as microporous insulation and Aerogel. The emissivity and  
51  
52 absorbtivity of the exposed surfaces is also accounted for.  
53  
54  
55  
56  
57

58 Different fin correlations can be chosen for the fluid channels. The choices include straight, offset, wavy, annular,  
59  
60 as well as other more specialized correlations. The shape of the fluid channels can also be specified as square  
61  
62  
63  
64  
65

1  
2 (rectangular), hexagonal, or circular. Radiation heat transfer is also computed with the convective heat transfer  
3  
4 coefficient within the fluid channels. Temperature dependent fluid properties for many different fluids are also part  
5  
6 of the model. The user can choose from air, water, glycol/water, helium/xenon, oil, exhaust gas, CO<sub>2</sub>, argon, as well  
7  
8 as other specialized fluids. The temperature dependent properties modeled include density, thermal conductivity,  
9  
10 specific heat, and dynamic viscosity.  
11

12  
13  
14  
15 Many different TE materials can be chosen for simulation, including Bi<sub>2</sub>Te<sub>3</sub>, PbTe, TAGS, half heusler, and  
16  
17 skutterudite. These materials can be chosen as single material or as a part of segmented TE elements. Material  
18  
19 properties, Seebeck coefficient, electrical resistivity, and thermal conductivity, as a function of temperature are taken  
20  
21 from measured data or are supplier-provided. To simulate improved TE materials, base TE material properties can  
22  
23 be scaled to a desired  $ZT_{avg}$ . The model allows the user to choose how this will occur, either by changing the  
24  
25 Seebeck coefficient, electrical resistivity, or thermal conductivity.  
26  
27

28  
29  
30  
31 The other materials of the device can also be chosen. This includes the materials for the fluid channel structures, the  
32  
33 connectors, and the fins, which may be different from the fluid channel. Material choices for these components  
34  
35 include copper, aluminum, different grades of SST, molybdenum, clad materials, and various ceramic materials. For  
36  
37 many of these materials, thermal and electrical conductivity are modeled as a function of temperature.  
38  
39  
40  
41

42  
43 The TE device can be broken up into multiple temperature banks in the direction of fluid flow. Each temperature  
44  
45 bank can have a separate set of TE elements. These elements can have different area to length aspect ratios, be  
46  
47 segmented differently with different TE materials, or not be segmented at all. Each temperature bank can operate on  
48  
49 its own electrical circuit or one electrical circuit can be used for all of the temperature banks. The temperature banks  
50  
51 can be of different lengths to better match the temperature gradients and heat flows in the direction of fluid flow. In  
52  
53 addition, each temperature bank can be modeled as having different hot side fin densities. This can be used to better  
54  
55 match the heat fluxes and temperatures seen in a particular bank. It also can help reduce the pressure drop and  
56  
57 weight of the fluid channel if lower density fins can be more advantageously used in different banks of the TEG.  
58  
59  
60  
61  
62  
63  
64  
65



Electrical load resistance affects the operating current and power output of the TEG at a particular set of temperature and heat flow conditions. Equation 2 shows how load resistance relates to operating current<sup>27</sup>.

$$I = \frac{\alpha \Delta T_{TE}}{R_{TE} + R_{load}}$$

### Equation 2

When designing the TEG for a particular set of temperature and heat flow conditions, the user will typically want to maximize the power output of the TEG. This condition occurs when the load resistance is equal to the internal resistance of the TEG. The model will also allow the user to run the model in off nominal conditions where the load resistance can be varied. This can be valuable in some designs since changing the current also affects the heat flow through the TE elements as can be seen in Equation 8.

To compute how all of the above attributes affect TEG operation, a set of energy balance equations have been defined.

$$Q_{h1} + \frac{1}{2} I^2 R_{conn,h} - UA_{TE-conn} (T_{cen,h} - T_{h1}) = 0$$

### Equation 3

$$Q_{h2} + \frac{1}{2} I^2 R_{conn,h} - UA_{TE-conn} (T_{cen,h} - T_{h2}) = 0$$

### Equation 4

$$UA_{TE-conn} (T_{cen,h} - T_{h1}) + UA_{TE-conn} (T_{cen,h} - T_{h2}) - UA_{cross,conn} (T_{sh2} - T_{cen,h}) = 0$$

### Equation 5

$$hA_h (T_{fh} - T_{sh2}) - UA_{cross,conn} (T_{sh2} - T_{cen,h}) - hA_{nat} (T_{sh2} - T_{\infty}) + UA_{cross,ch,h,1-2} (\Delta T_{sh1}) - UA_{cross,ch,h,2-3} (\Delta T_{sh2}) = 0$$

### Equation 6

$$\dot{m} C p_h \Delta T_{fh} - hA_h (T_{fh} - T_{sh2}) = 0$$

### Equation 7

1  
2  
3  
4  
5  
6  
7  
8  
9  
10  
11  
12  
13  
14  
15  
16  
17  
18  
19  
20  
21  
22  
23  
24  
25  
26  
27  
28  
29  
30  
31  
32  
33  
34  
35  
36  
37  
38  
39  
40  
41  
42  
43  
44  
45  
46  
47  
48  
49  
50  
51  
52  
53  
54  
55  
56  
57  
58  
59  
60  
61  
62  
63  
64  
65

Where

$$Q_h = \alpha IT_h + K\Delta T_{TE} - \frac{1}{2}I^2(R_{TE} + 2R_{int})$$

**Equation 8**

Equation 3 and Equation 4 are energy balance equations for conductive heat transfer from the TE elements into the connectors. Equation 5 and Equation 6 are energy balance equations for conductive heat transfer from the connector through the fluid-carrying channel wall through the fins to fluid convective heat transfer. They include the losses due to natural convection, radiation, and Joule heating of the boxes. Equation 7 is an energy balance equation for the convective heat transfer into the fluid. Equation 8 is the basic equation for thermoelectric heat flow in power generation.

The model solves these governing equations simultaneously for steady-state temperatures at each node in the direction of flow using the FMINCON function in MATLAB. The number of simultaneous equations varies with the number of TE elements in the direction of fluid flow.

Outputs for the model include power output, efficiency, hot and cold outlet temperatures, hot and cold pressure drops, total mass and volume, and many others. Auxiliary power of pumps and/or fans is also computed based on the pressure drops. This output can be used to calculate a net power output instead of gross power.

Some validation has been completed for this model for low temperature (<250C) devices using single material elements with liquid heat exchangers as reported in Crane et al.<sup>19</sup>. The error from measurement to model was <10%. Further validation is needed on the integration of segmented elements into gas/liquid heat exchangers.

Optimization

1  
2  
3  
4 Advanced multi-parameter optimization can be used on the steady state model for better understanding of the  
5  
6 interactions between various design variables and parameters and to further improve the performance of the design.  
7  
8 The TEG design problem, an example of a constrained, non-linear, minimization problem, is solved using the  
9  
10 MATLAB function FMINCON, which uses a gradient-based optimization scheme.  
11  
12  
13  
14

15 A design engineer can choose to optimize from greater than 20 different design variables, including fin and TE  
16  
17 dimensions and include dozens of different design parameters. A variety of different constraints can also be chosen,  
18  
19 including minimum power density, maximum hot- and cold-side pressure drops, maximum total mass, and minimum  
20  
21 output power. Constraints can also be placed on maximum TE surface temperatures and maximum temperature  
22  
23 gradients across the TE elements to help improve design robustness. The objective function of the analysis can also  
24  
25 be chosen. Choices include maximum gross or net power, maximum efficiency, and maximum gross or net power  
26  
27 density, which can be based on either total mass or TE mass. Once the design variables, parameters, constraints, and  
28  
29 objective function have been chosen, an optimization analysis can be conducted. The result is a nominal design that  
30  
31 can now be used in an operating model where the design conditions can vary.  
32  
33  
34  
35  
36  
37  
38  
39

#### 40 Transient Model Development 41 42 43

44 The steady state model gives an effective means to choose a nominal design point and optimize the design for this  
45  
46 set of operating conditions. However, a thermoelectric generator often may see a wide array of operating conditions,  
47  
48 and these conditions may change frequently as a function of time. This is certainly the case when the TEG is  
49  
50 integrated into a car or truck. An example of the mass flows and temperatures in the exhaust system, downstream of  
51  
52 the catalytic converter, that are produced for an automotive city drive cycle (FTP-75) are shown in Figure 3. The  
53  
54 thermal time constants of the exhaust system and of the TEG itself can have a large effect on how the TEG performs  
55  
56 in this cycle.  
57  
58  
59  
60  
61  
62  
63  
64  
65

1  
2  
3  
4 In order to model the TEG in different cycles as well as other non-steady state operating conditions, the steady state  
5 models for TE couples and devices were adapted into transient models. To do this, the energy balance equations  
6 defined above were setup as differential equations based on Equation 9 and integrated into the S- Function template  
7 of MATLAB/Simulink..  
8

$$mC_p \frac{dT}{dt} = Q_1 - Q_2$$

### Equation 9

19  
20 The  $mC_p$  term in Equation 9 is the thermal mass of each control volume that the equation represents. This could be  
21 a fluid, heat exchanger, connector, or TE thermal mass depending on the control volume. It is important to  
22 determine the direction of heat flow to make sure that the signs for  $Q_1$  and  $Q_2$  are correct. Otherwise, the differential  
23 equations will not be able to be solved correctly.  
24  
25  
26  
27

28  
29  
30  
31 When using Simulink to solve ordinary differential equations, there is a choice of solvers made available to the user.  
32  
33 Due to the potential rapid variation in the solution of the differential equations, the transient TEG problem is  
34 considered stiff. Ode15s, specifically designed to handle stiff problems, is the solver that most successfully solved  
35 the set of differential equations for the transient TEG problem.  
36  
37  
38

39  
40  
41  
42 A transient model was first setup for the TE couple. A validation experiment was conducted using segmented  
43 elements on a heater housing, cooled between two small cold plates. The heater housing holds a cartridge heater,  
44 which was used to provide heat to the couple. This couple setup was similar to that described in Crane et al.<sup>16</sup> for  
45 the 10% efficient generator. The segmented elements were made up of TAGS/PbTe and Bi<sub>2</sub>Te<sub>3</sub>. Graphs of the test  
46 results can be seen in the figure below.  
47  
48  
49  
50  
51  
52

53  
54  
55  
56 The test was setup where the cartridge heater was held at a constant heat input of 35W. The hot side temperature of  
57 the TE elements was 500C and the cold water bath was set at 20C. The electrical load resistance was initially  
58 infinite making the initial current zero by Equation 2. Then the electrical load resistance was instantly changed to  
59  
60  
61  
62  
63  
64  
65

1  
2 30A. The electrical time constants of the couple were much faster than the thermal time constants. Thus, spikes in  
3  
4 power and efficiency can be seen in the graphs before the thermal time constants catch up to the electrical time  
5  
6 constants.  
7  
8  
9

10  
11 By adjusting the electrical load resistance, the electrical current is instantly increased. This increases the effective  
12  
13 thermal conductivity of the elements by Equation 8. The original temperature differences of the couple no longer  
14  
15 balance the steady state equations. The time it takes to balance these temperature differences with the new effective  
16  
17 thermal conductance of the couple is based on the thermal mass of the elements and their connectors. This can  
18  
19 clearly be seen in the graphs. Greater power output and efficiency are achieved initially due to the couple operating  
20  
21 at higher temperature differences at the same heat flow. The higher temperature differences increase open circuit  
22  
23 voltage and subsequently power output. They also increase the Carnot term of the TEG efficiency. However, these  
24  
25 temperature differences are not sustainable in steady state, and thus the power output and efficiency eventually come  
26  
27 down.  
28  
29  
30

31  
32  
33 The cold side temperature initially increases due to the sudden increase in effective thermal conductance,  
34  
35 transferring more heat from the hot to cold side of the TE elements. This is also what causes the hot side  
36  
37 temperature to decrease. As the system balances, it stabilizes at a more inbetween temperature in this example. The  
38  
39 figures show excellent correlation between the measured and simulated data, where differences are <5%.  
40  
41  
42  
43

44  
45 With this validation, a transient model was created of the TEG itself, TE couples integrated directly into the heat  
46  
47 exchangers. The optimized design from the steady state model is used as a baseline. Inputs for the model are  
48  
49 similar to those of the steady state model. Operating condition inputs include the hot and cold side inlet  
50  
51 temperatures and flows and the electrical load resistance. The electrical load resistance can be set to be always equal  
52  
53 to the internal resistance of the TEG or it can be set at a particular constant load. A controller simulator can be  
54  
55 attached to the model as an additional Simulink block in order to simulate the effects of a varying electrical load that  
56  
57 is not necessarily optimal. Outputs for the model are again similar to those of the steady state model.  
58  
59  
60  
61  
62  
63  
64  
65

1  
2 The model can be operated as is in a stand-alone mode or the S-function can be cut and pasted into a larger systems-  
3  
4 level model. Both BMW and Ford have cut and pasted versions of this model into their larger systems-level  
5  
6 models<sup>18</sup>. The model can be run using single hot-side inlet flow and temperature conditions or using the hot-side  
7  
8 inlet flow and temperature conditions for a drive cycle.  
9

10  
11  
12  
13 Additional systems level attributes have been added to the transient model to aid in its use as a part of a larger  
14  
15 system. A maximum hot inlet temperature can be defined to prevent the overheating of the TE elements or any other  
16  
17 part of the TEG device. A maximum hot flow can be defined to prevent excessive backpressure in the system. This  
18  
19 excessive backpressure can reduce engine performance if the TEG is integrated into the exhaust system of a vehicle.  
20  
21 In addition, to better match the thermal impedance of a dynamic thermal system as defined in Crane and Bell<sup>20</sup>, the  
22  
23 TEG can be broken into a number of TE sections. Having multiple TE sections can allow the TEG to operate better  
24  
25 at low flows when the design has been optimized for higher flow rates.  
26  
27  
28  
29  
30

31 Below are examples of transient simulations done with the model. Figure 5 shows the power output and hot side  
32  
33 fluid and TE surface temperatures for the TEG being driven by a set of constant operating conditions towards steady  
34  
35 state from an initial set of conditions. The temperature curves in these figures are at different positions in the  
36  
37 direction of flow in the TEG as a function of time. The colder the temperatures the further they are from the inlet of  
38  
39 the TEG. Figure 6 shows the power output and efficiency along with the hot side fluid and TE surface temperatures  
40  
41 for the TEG for an FTP-75 (city) automotive drive cycle.  
42  
43  
44  
45  
46  
47  
48

## 49 Conclusion

50  
51  
52  
53

54 Steady state and transient models of thermoelectric devices have been introduced that range from element to couple  
55  
56 to device to system level. Equations for these models have been described, and validation studies have been  
57  
58 discussed. Further validation is needed for the gas/liquid TEG with segmented TE elements. Next steps include the  
59  
60 testing of the newly designed and built cylindrical TEG, which is designed for hot exhaust gas on one side and  
61  
62  
63  
64  
65

1  
2 automotive coolant on the other. It also includes segmented TE elements. Once tested, empirical results can be  
3  
4 compared to steady state and transient simulations for a more complete model validation.  
5  
6  
7  
8

9 With this further validation, a very powerful set of validated tools will exist that can greatly aid in the design of  
10  
11 future thermoelectric power generation devices and systems. The tools have already been used by multiple  
12  
13 customers to help in their design process. Hopefully, many more will use them in the future as well.  
14  
15  
16  
17  
18  
19

## 20 Acknowledgements

21  
22  
23  
24

25 The author would like to thank John Fairbanks and the US Department of Energy Office of Vehicle Technologies  
26  
27 for their support and funding for much of the work relating to this paper; Carl Maronde from DOE NETL for project  
28  
29 management; Andreas Eder and Boris Mazar from BMW and Clay Maranville from Ford for their valued support as  
30  
31 project team members; Jeff Snyder from Caltech for consultation on modeling segmented elements; John  
32  
33 LaGrandeur from BSST for his overall project management and support; Steve Ayers from BSST for heat exchanger  
34  
35 modeling consultation; and Lon Bell from BSST for his overall consultation and inspiration without which this work  
36  
37 could not have been completed  
38  
39  
40  
41  
42  
43  
44

## 45 Nomenclature

46  
47  
48  
49

50	A	area ( $m^2$ )
51		
52	Cp	specific heat (J/kgK)
53		
54	h	heat transfer coefficient ( $W/m^2K$ )
55		
56	I	electrical current (A)
57		
58	K	thermal conductance (W/K)
59		
60	m	mass (kg)
61		
62		
63		
64		
65		

1  
2  
3  
4  
5  
6  
7  
8  
9  
10  
11  
12  
13  
14  
15  
16  
17  
18  
19  
20  
21  
22  
23  
24  
25  
26  
27  
28  
29  
30  
31  
32  
33  
34  
35  
36  
37  
38  
39  
40  
41  
42  
43  
44  
45  
46  
47  
48  
49  
50  
51  
52  
53  
54  
55  
56  
57  
58  
59  
60  
61  
62  
63  
64  
65

Q heat flow (W)  
R electrical resistance (ohm)  
t time (s)  
T temperature (K)  
u reduced current density  
U overall heat transfer coefficient (W/m<sup>2</sup>K)

*Subscripts*

1, 2, 3 location on the TEG/control volume in the direction of flow  
c cold  
cen center of  
ch channel  
conn connector  
cross cross sectional  
f fluid  
h hot  
int interfacial  
load load  
nat natural convection  
s surface  
TE thermoelectric

*Greek letters*

$\alpha$  Seebeck coefficient  
 $\Delta, d$  change in  
 $\infty$  ambient



1  
2  
3  
4  
5  
6  
7  
8  
9  
10  
11  
12  
13  
14  
15  
16  
17  
18  
19  
20  
21  
22  
23  
24  
25  
26  
27  
28  
29  
30  
31  
32  
33  
34  
35  
36  
37  
38  
39  
40  
41  
42  
43  
44  
45  
46  
47  
48  
49  
50  
51  
52  
53  
54  
55  
56  
57  
58  
59  
60  
61  
62  
63  
64  
65

## References

1. Ebling, D., et al., *Multiphysics Simulation of Thermoelectric Systems for Comparison with Experimental Device Performace*. Journal of Electronic Materials, 2009. **38**(7): p. 1456-1461.
2. Lau, P.G. and R.J. Buist. *Calculation of Thermoelectric Power Generation Performance Using Finite Element Analysis*. in *16th International Conference on Thermoelectrics*. 1997. Dresden, Germany: IEEE.
3. Antonova, E.E. and D.C. Looman. *Finite Elements for Thermoelectric Device Analysis in ANSYS*. in *International Conference on Thermoelectrics*. 2005. Clemson, SC: IEEE.
4. Chen, M., et al. *Multi-physics Simulation of Thermoelectric Generators Through Numerically Modeling*. in *International Conference on Thermoelectrics*. 2007. JeJu Island, South Korea: IEEE.
5. Chen, M., et al. *Transient Behavior Study of Thermoelectric Generators through an Electro-thermal Model Using SPICE*. in *International Conference on Thermoelectrics*. 2006. Vienna, Austria: IEEE.
6. Mitrani, D., et al., *One-dimensional modeling of TE devices considering temperature-dependent parameters using SPICE*. Microelectronics Journal, 2009. **40**(9): p. 1398-1405.
7. Hendricks, T.J. and J.A. Lustbader. *Advanced Thermoelectric Power System Investigations for Light-Duty and Heavy Duty Applications: Part I*. in *21st International Conference on Thermoelectrics*. 2002. Long Beach, CA: IEEE.
8. Hendricks, T.J. and J.A. Lustbader. *Advanced Thermoelectric Power System Investigations for Light-Duty and Heavy Duty Applications: Part II*. in *21st International Conference on Thermoelectrics*. 2002. Long Beach, CA: IEEE.
9. Saber, H.H. and M.S. El-Genk. *Optimization of Segmented Thermoelectric for Maximizing Conversion Efficiency and Electric Power Density*. in *21st International Conference on Thermoelectrics*. 2002. Long Beach, CA: IEEE.
10. Hendricks, T.J., *Thermal System Interactions in Optimizing Advanced Thermoelectric Energy Recovery*. Journal of Energy Resources Technology, 2007. **129**(September 2007): p. 223-231.
11. Hendricks, T.J. and N.K. Karri. *Design Impacts of Stochastically-Varying Input Parameters on Advanced Thermoelectric Conversion Systems*. in *International Conference on Thermoelectrics*. 2007. JeJu Island, South Korea: IEEE.
12. Hendricks, T.J. and N.K. Karri. *Probabilistic design & analysis for robust design of advanced thermoelectric conversion systems*. in *Energy Sustainability Conference*. 2007. Long Beach, CA: ASME.
13. Crane, D.T., *Optimizing Thermoelectric Waste Heat Recovery from an Automotive Cooling System*. 2003, University of Maryland, College Park: College Park, MD.

- 1
- 2 14. Crane, D.T. and G.S. Jackson, *Optimization of Cross Flow Heat Exchangers for Thermoelectric Waste Heat Recovery*.
- 3
- 4 Energy Conversion and Management, 2004. **45**(9-10): p. 1565-1582.
- 5
- 6 15. Crane, D.T. *Modeling High-Power Density Thermoelectric Assemblies Which Use Thermal Isolation*. in *23rd*
- 7
- 8 *International Conference on Thermoelectrics*. 2004. Adelaide, AU.
- 9
- 10 16. Crane, D.T., D. Kossakovski, and L.E. Bell, *Modeling the Building Blocks of a 10% Efficient Segmented*
- 11
- 12 *Thermoelectric Power Generator*. Journal of Electronic Materials, 2009. **38**(7): p. 1382.
- 13
- 14 17. Crane, D.T. and L.E. Bell. *Progress Towards Maximizing the Performance of a Thermoelectric Power Generator*. in
- 15
- 16 *25th International Conference on Thermoelectrics*. 2006. Vienna, Austria: IEEE.
- 17
- 18 18. Crane, D.T., J.W. LaGrandeur, and L.E. Bell. *Progress Report on BSST Led, US DOE Automotive Waste Heat*
- 19
- 20 *Recovery Program*. in *International Conference on Thermoelectrics*. 2009. Freiburg, Germany.
- 21
- 22 19. Crane, D.T., et al., *Performance Results of a High Power Density Thermoelectric Generator: Beyond the Couple*.
- 23
- 24 Journal of Electronic Materials, 2009. **38**(7): p. 1375.
- 25
- 26 20. Crane, D.T. and L.E. Bell, *Design to Maximize Performance of a Thermoelectric Power Generator With a Dynamic*
- 27
- 28 *Thermal Power Source*. Journal of Energy Resources Technology, 2009. **131**(March 2009).
- 29
- 30 21. Bell, L.E. *High Power Density Thermoelectric Systems*. in *23rd International Conference on Thermoelectrics*. 2004.
- 31
- 32 Adelaide, AU.
- 33
- 34 22. Bell, L.E. and D.T. Crane. *Vehicle Waste Heat Recovery System Design and Characterization*. in *International*
- 35
- 36 *Thermoelectric Conference*. 2009. Freiburg, Germany.
- 37
- 38 23. Snyder, G.J., *Thermoelectric Power Generation: Efficiency and Compatibility*, in *Thermoelectrics Handbook Macro*
- 39
- 40 *To Nano*, D.M. Rowe, Editor. 2006, CRC Press: Boca Raton, FL. p. 9-1 - 9-26.
- 41
- 42 24. Nolas, G.S., J. Sharp, and H.J. Goldsmid, *Thermoelectrics - Basic Principles and New Materials Developments*. 2001,
- 43
- 44 Berlin Heidelberg: Springer-Verlag.
- 45
- 46 25. Rohsenow, W.M., J.P. Hartnett, and Y.I. Cho, eds. *Handbook of Heat Transfer*. 3rd ed. 1998, McGraw-Hill: New
- 47
- 48 York, NY.
- 49
- 50 26. Faulkner, F., *COLDPLT.exe*. 1999, Thermodynamics Analysis Service: Hobe Sound, FL.
- 51
- 52 27. Angrist, S.W., *Direct Energy Conversion*. 4th ed. 1982, Boston: Allyn and Bacon, Inc.
- 53
- 54
- 55
- 56
- 57
- 58
- 59
- 60
- 61
- 62
- 63
- 64
- 65

## Figure

[Click here to download Figure: figure captions ICT2010.docx](#)

**Figure 1. TEG high power density subassembly**

Figure 2. Schematic of TE subassembly with heat exchangers (HEX) showing temperature locations in the model.

**Figure 3.** Exhaust gas mass flow and temperature exiting the catalytic converter varying with time for the FTP-75 drive cycle for an inline 6 cylinder engine with 3.0L displacement.

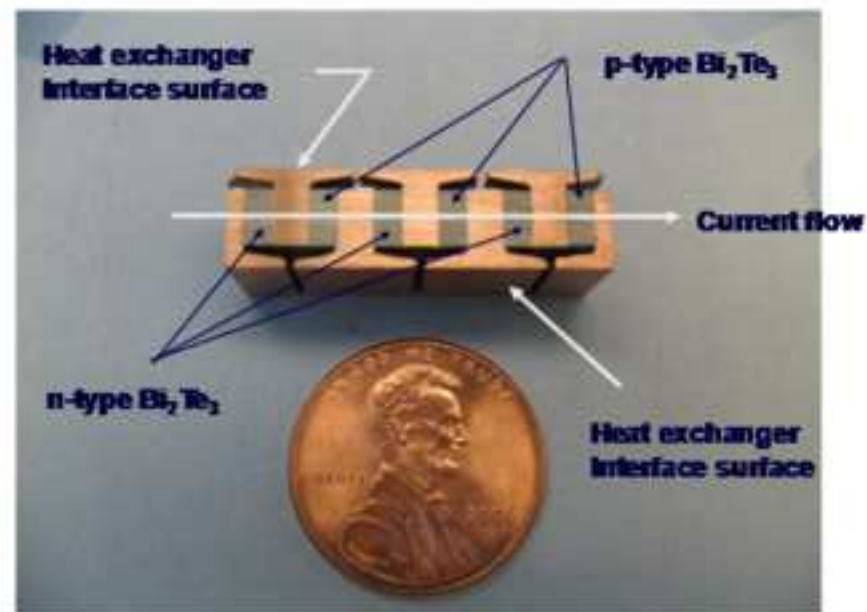
**Figure 4. Transient experimental and simulated performance of a TE couple.**

**Figure 5. Simulated outputs for the transient TEG model using constant operating conditions.**

**Figure 6. Simulated outputs for the automotive FTP-75 drive cycle using an optimized TEG from the steady state model.**

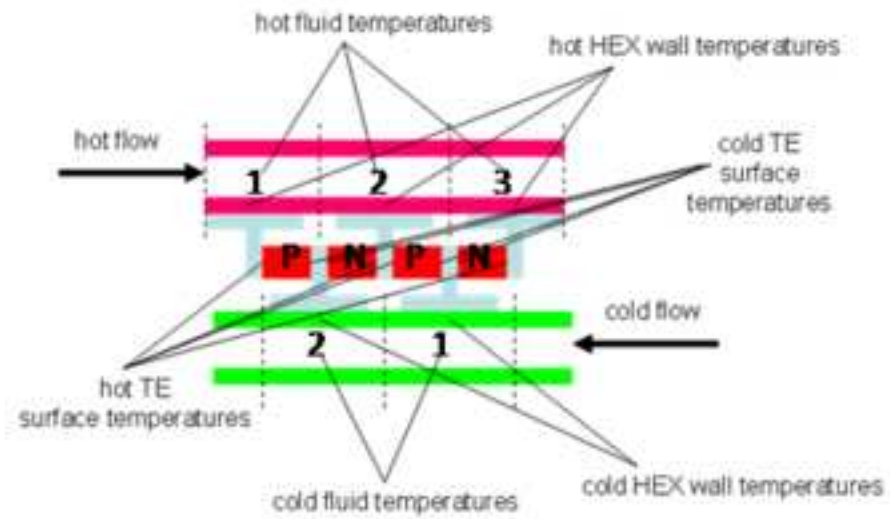
Figure

[Click here to download high resolution image](#)



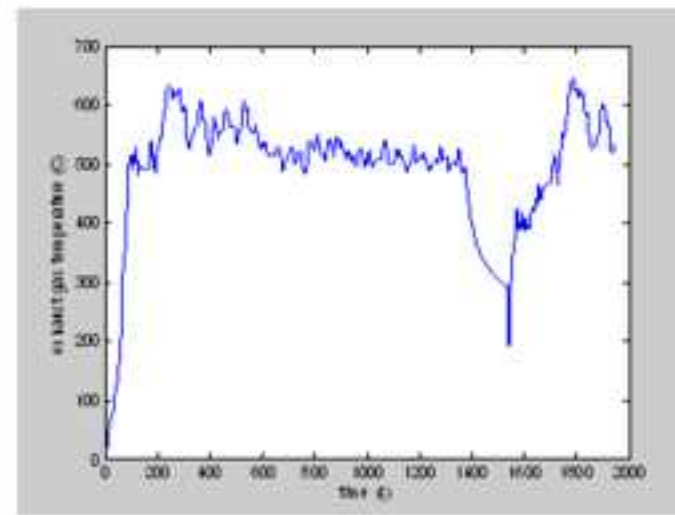
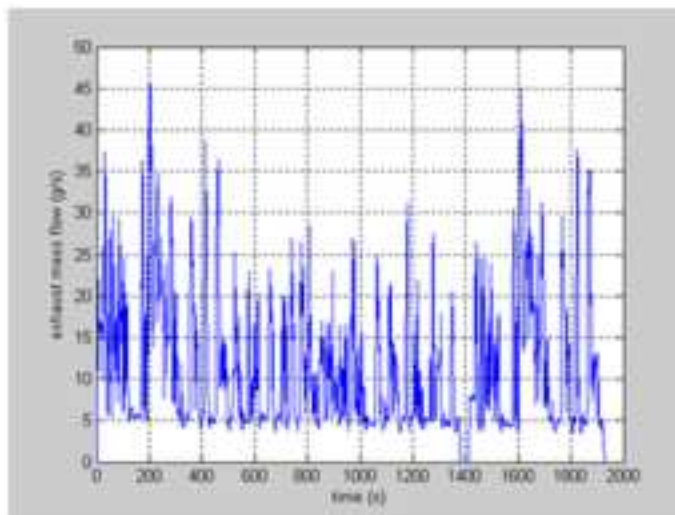
Figure

[Click here to download high resolution image](#)



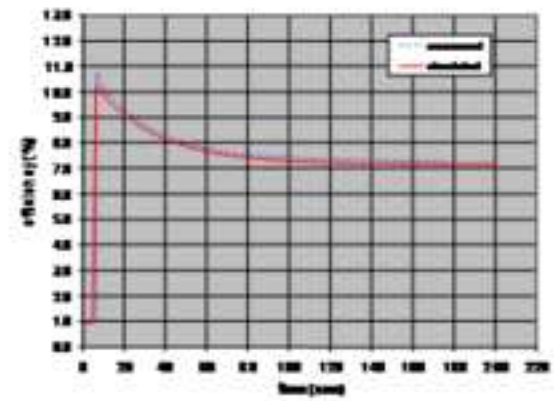
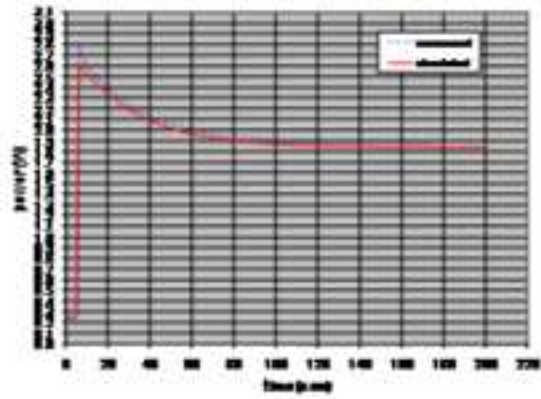
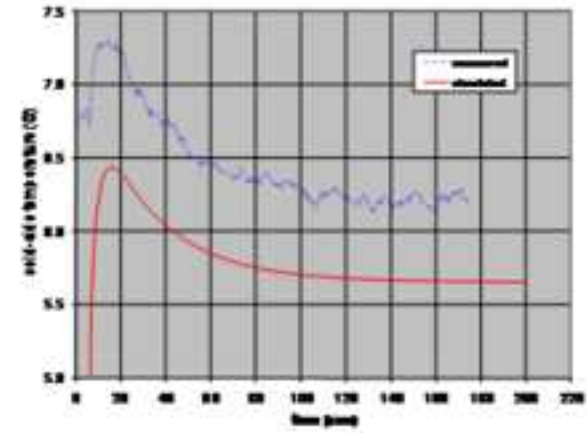
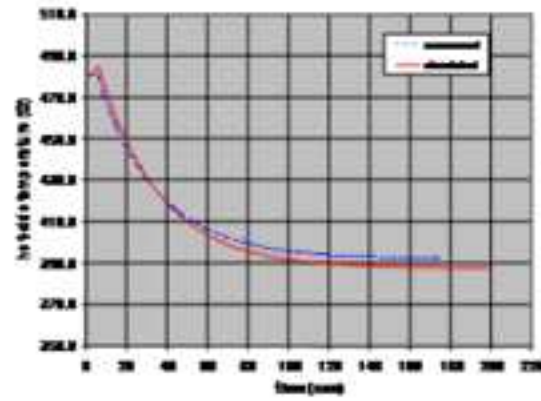
# Figure

[Click here to download high resolution image](#)



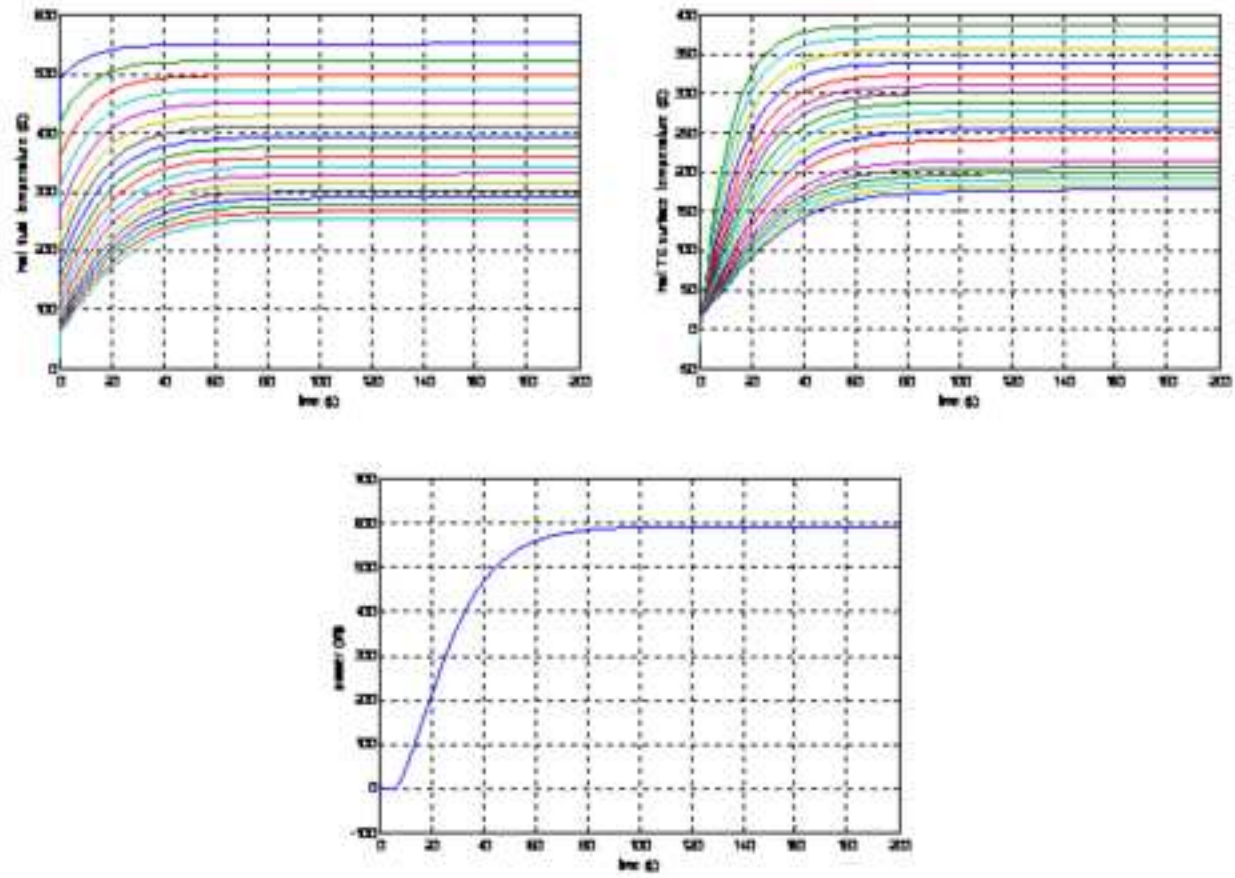
Figure

[Click here to download high resolution image](#)



Figure

[Click here to download high resolution image](#)





# Figure

[Click here to download high resolution image](#)

